

# Circular dichroism in angle-resolved photoemission spectrum: computational approach


M. Lindroos  
Tampere University of  
Technology  
Tampere, Finland

# OUTLINE

- ❑ Introduction and general remarks on role of the circular polarization in ARPES matrix elements.
- ❑ Proofs that we can compute Dichromatic Signals ( $D_S$ ) and experiments agree with us.
- ❑ Applying our methods for Bi2212 and the role of geometric details of the crystals on  $D_S$ .
- ❑ Graphene
- ❑ Au(111)
- ❑ Conclusions

# The one step equation for photoemission intensity

$$I(\mathbf{k}_{||}, \epsilon_f) = -\frac{1}{\pi} \Im \langle \mathbf{k}_{||}, \epsilon_f | G_2^+ \Delta G_1^+ \Delta^\dagger G_2^- | \mathbf{k}_{||}, \epsilon_f \rangle$$



For group theoretical purposes:

$$-\frac{1}{\pi} \Im G_1^+ = \sum_i B_{ii} |i\rangle \langle i|, \quad \longrightarrow \quad I(\mathbf{k}_{||}, \epsilon_f) = \sum_i B_{ii} |\langle f | \Delta | i \rangle|^2.$$

$$\Delta = \frac{\mathbf{A} \cdot \mathbf{p}}{c} = \frac{\mathbf{A} \cdot \nabla V}{\omega c}$$

$$\mathbf{A} = \frac{\mathbf{a}}{2} e^{i\mathbf{q} \cdot \mathbf{r}} = a \frac{\hat{\mathbf{e}}}{2} e^{i\mathbf{q} \cdot \mathbf{r}}$$

$$\hat{\mathbf{e}} = \hat{\mathbf{x}}' - i\hat{\mathbf{y}}' \quad (\text{LH})$$

$$\hat{\mathbf{e}} = \hat{\mathbf{x}}' + i\hat{\mathbf{y}}' \quad (\text{RH})$$

The dichroism signal  $D_S$  that is the difference between intensity for left- and righthanded polarization is

$$\begin{aligned}
 D_S &= I_{\text{RH}} - I_{\text{LH}} = \\
 &\frac{a^2}{8c^2} \sum_i B_{ii} \left[ |\langle f | (\hat{\mathbf{x}}' + i\hat{\mathbf{y}}') \cdot \mathbf{p} | i \rangle|^2 - |\langle f | (\hat{\mathbf{x}}' - i\hat{\mathbf{y}}') \cdot \mathbf{p} | i \rangle|^2 \right] \\
 &= -\frac{a^2}{2c^2} \sum_i B_{ii} \Im \{ \langle i | \hat{\mathbf{x}}' \cdot \mathbf{p} | f \rangle \langle f | \hat{\mathbf{y}}' \cdot \mathbf{p} | i \rangle \} . \quad (7)
 \end{aligned}$$

If final state is treated as plane wave the product of the two matrix elements is real and  $D_s$  is always zero !

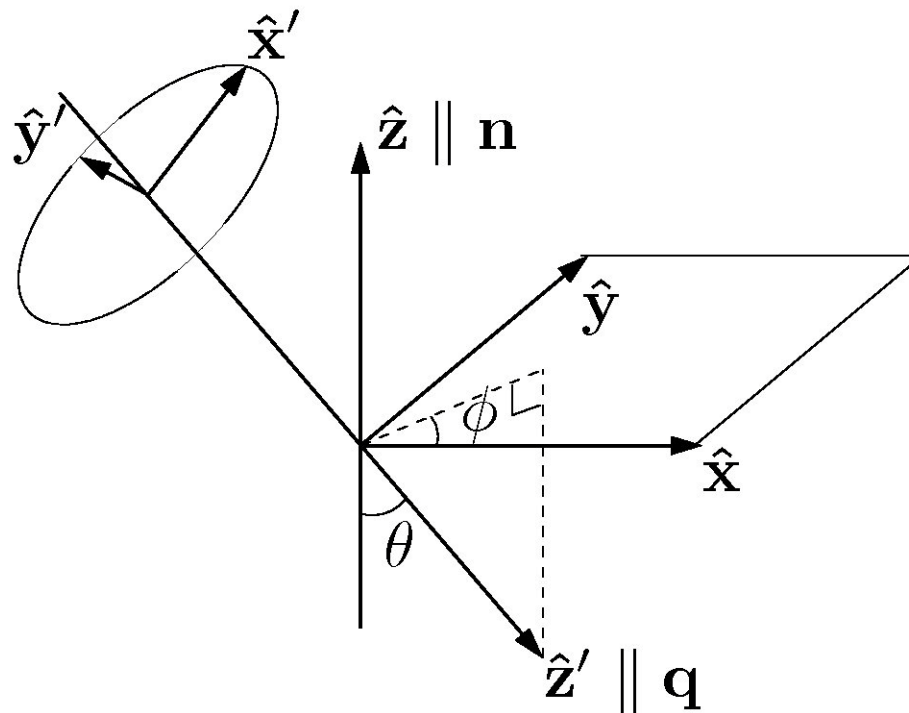
If wavevector of the incident photon and the photoelectron lie on a mirror or a glide plane either  $\langle i | \hat{\mathbf{x}}' \cdot \mathbf{p} | f \rangle$  or  $\langle i | \hat{\mathbf{y}}' \cdot \mathbf{p} | f \rangle$  is zero. To get nonzero intensity mirror symmetry must be broken!!

From a coordinate system of the photon to coordinates of the crystal

$$\hat{\mathbf{x}}' = \cos(\phi) \cos(\theta) \hat{\mathbf{x}} + \sin(\phi) \cos(\theta) \hat{\mathbf{y}} + \sin(\theta) \hat{\mathbf{z}}$$

$$\hat{\mathbf{y}}' = -\sin(\phi) \hat{\mathbf{x}} + \cos(\phi) \hat{\mathbf{y}},$$

$$\hat{\mathbf{z}}' = \cos(\phi) \sin(\theta) \hat{\mathbf{x}} + \sin(\phi) \sin(\theta) \hat{\mathbf{y}} - \cos(\theta) \hat{\mathbf{z}}.$$

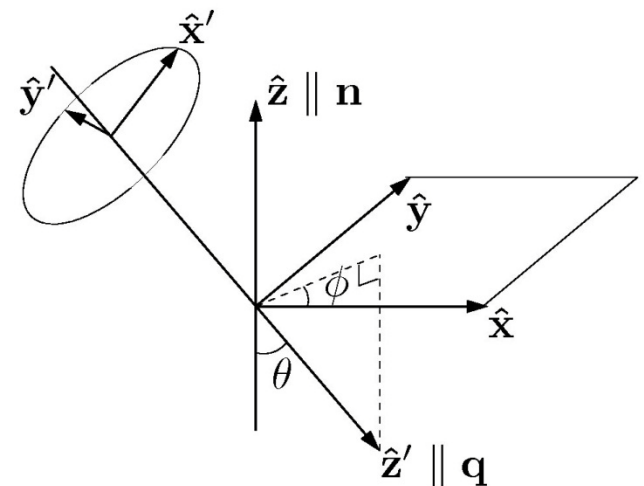


Thus in general incidence for dichroism signal

$$D_S = -\frac{a^2}{2c^2} \sum_i B_{ii} \Im \left\{ \cos \phi \sin \theta M_{fi}^{(z)} M_{if}^{(y)} \right. \\ \left. - \sin \phi \sin \theta M_{fi}^{(z)} M_{if}^{(x)} + \cos \theta M_{fi}^{(x)} M_{if}^{(y)} \right\}$$

$$M_{if}^{(j)} = \langle f | \hat{\mathbf{j}} \cdot \mathbf{p} | i \rangle, \quad \mathbf{j} = \mathbf{x}, \mathbf{y}, \mathbf{z}$$

That's an end for easy interpretations  
and what about robustness...



## Angular dependence of circular dichroism in Bi2212

V. Arpiainen<sup>1</sup>, V. Zalobotnyy<sup>2</sup>, A. A. Kordyuk<sup>2,3</sup>, S. V. Borisenko<sup>2</sup>, M. Lindroos<sup>1</sup>

<sup>1</sup>*Institute of Physics, Tampere University of Technology, P.O. Box 692, FIN-33101 Tampere, Finland*

<sup>2</sup>*Leibniz-institute for Solid State Research, IFW-Dresden, P.O. Box 270116, D-01171 Dresden, Germany*

<sup>3</sup>*Institute of Metal Physics of National Academy of Sciences of Ukraine, 03142 Kyiv, Ukraine*

(Dated: October 4, 2007)

We have investigated both experimentally and computationally ARPES spectra of  $\text{Bi}_2\text{Sr}_2\text{CaCu}_2\text{O}_{8+\delta}$  and  $(\text{BiPb})_2\text{Sr}_2\text{CaCu}_2\text{O}_{8+\delta}$  with circularly polarized light. The large circular dichroism in the angular distribution of photoelectrons is reproduced by non-magnetic one-step calculations within dipole approximation. A strong dependence of spectral weight on experimental parameters, especially on excitation energy, is found.

Phys. Rev. B77 (2008)024520.

$$D_S = I_{RH} - I_{LH}$$

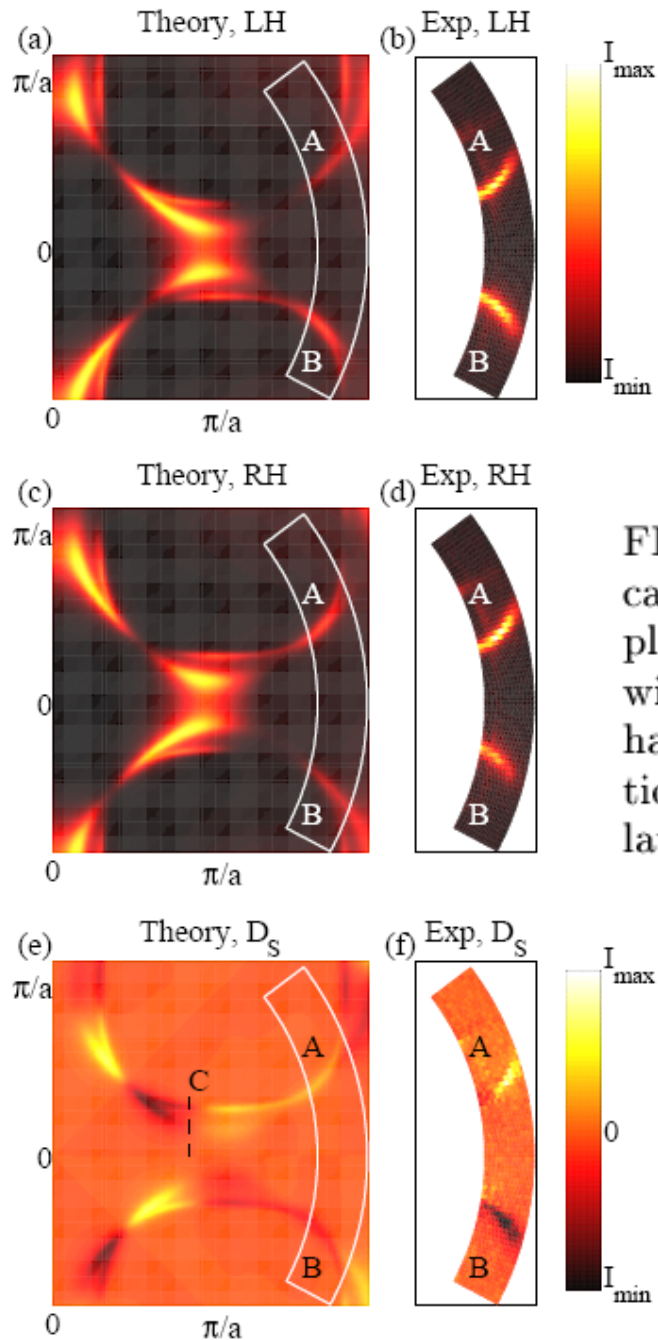


FIG. 3: Comparison between experimental and theoretical FS maps, normal incidence setup,  $h\nu = 20$  eV, sample  $(\text{BiPb})_2\text{Sr}_2\text{CaCu}_2\text{O}_{8+\delta}$  with  $T_c = 72\text{K}$ . (a) Calculated with left-handed circular polarization. (b) Experiment, left-handed polarization. (c) Calculated, right-handed polarization. (d) Experiment, right-handed polarization (e) Calculated dichroism signal. (f) Experiment, dichroism signal.

A very good level of agreement between theory and experiments.



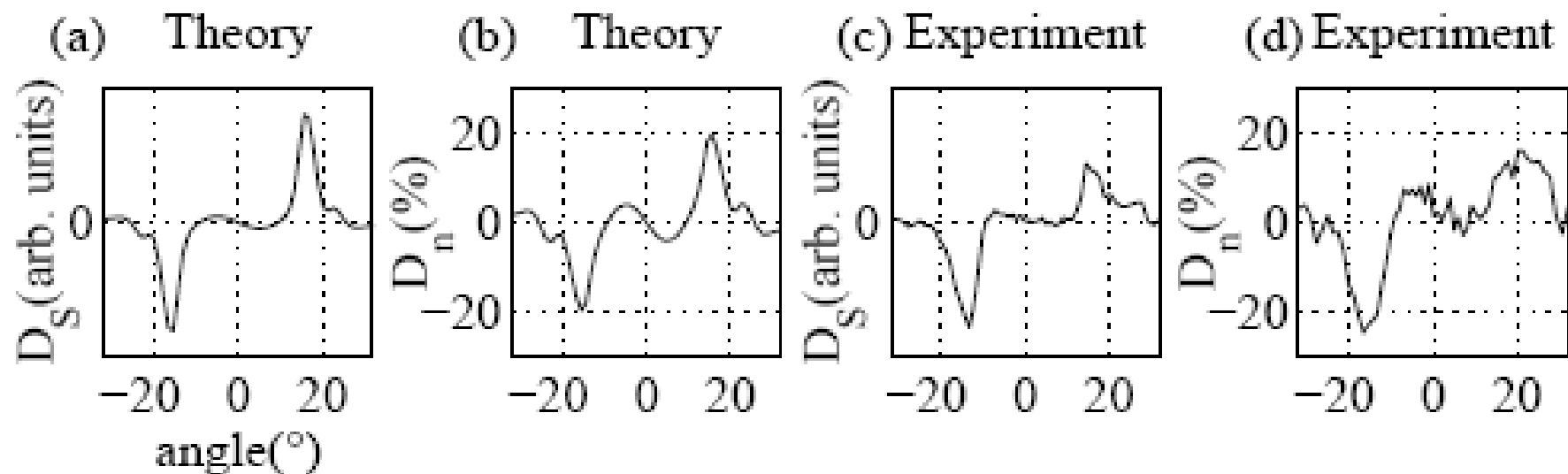
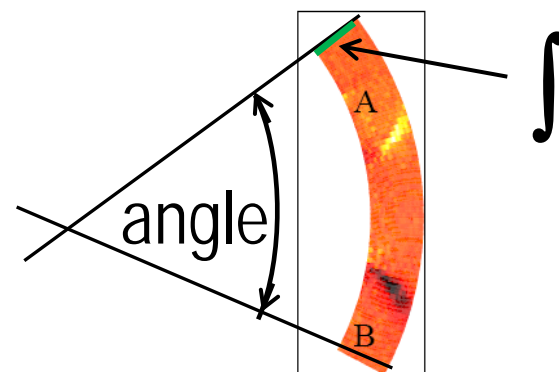


FIG. 4: Dichroism signals  $D_S$  and normalized  $D_n$  integrated through the experimentally probed part of  $k_{||}$ -space in Fig. 3 and plotted as a function of electron's escape angle. (a) Calculated  $D_S$ . (b) Calculated  $D_n$ . (c) Experimental  $D_S$ . (d) Experimental  $D_n$ .

$$D_n = \frac{(I_{RH} - I_{LH})}{(I_{RH} + I_{LH})}$$



$D_S$  depends strongly on photon energy.

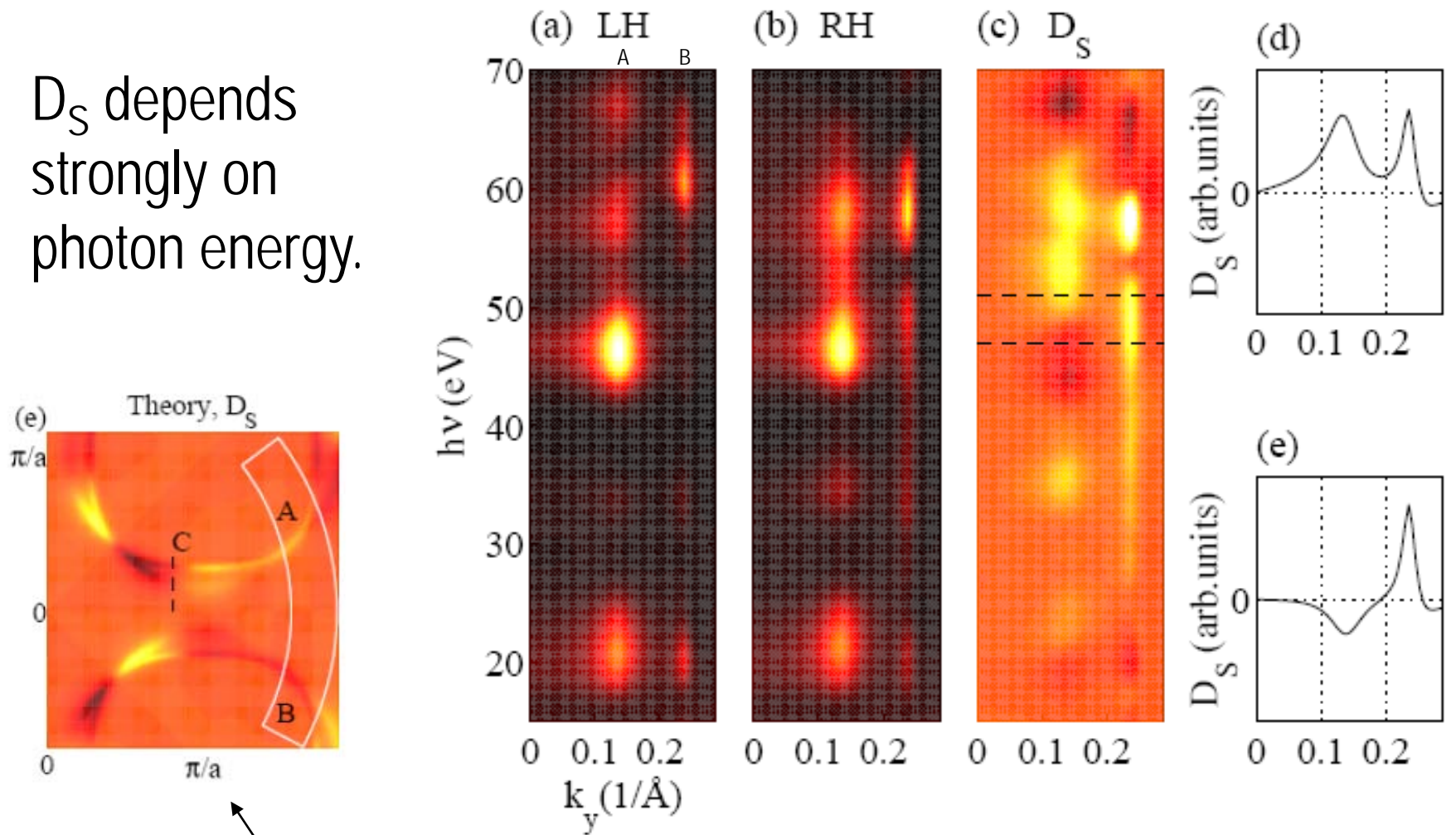


FIG. 7: Photoelectron intensity calculated as a function of excitation energy at  $k_x = 0.66$   $1/\text{\AA}$  along the dashed line labeled with C in Fig. 3e. (a) LH light. (b) RH light. (c) Map of  $D_S$ . (d) MDC of  $D_S$  at  $h\nu = 51$  eV, along upper dashed line in subfigure c. (e) MDC of  $D_S$  at  $h\nu = 47$  eV, along lower dashed line in subfigure c.

# Dichroic effects due to orthorhombic distortions

PRL 103, 067005 (2009)

PHYSICAL REVIEW LETTERS

week ending  
7 AUGUST 2009

## Circular Dichroism in the Angle-Resolved Photoemission Spectrum of the High-Temperature $\text{Bi}_2\text{Sr}_2\text{CaCu}_2\text{O}_{8+\delta}$ Superconductor: Can These Measurements Be Interpreted as Evidence for Time-Reversal Symmetry Breaking?

V. Arpiainen,<sup>1</sup> A. Bansil,<sup>2</sup> and M. Lindroos<sup>1,2</sup>

<sup>1</sup>*Department of Physics, Tampere University of Technology, P.O. Box 692, FIN-33101 Tampere, Finland*

<sup>2</sup>*Department of Physics, Northeastern University, Boston, Massachusetts 02115, USA*

(Received 18 November 2008; published 5 August 2009)

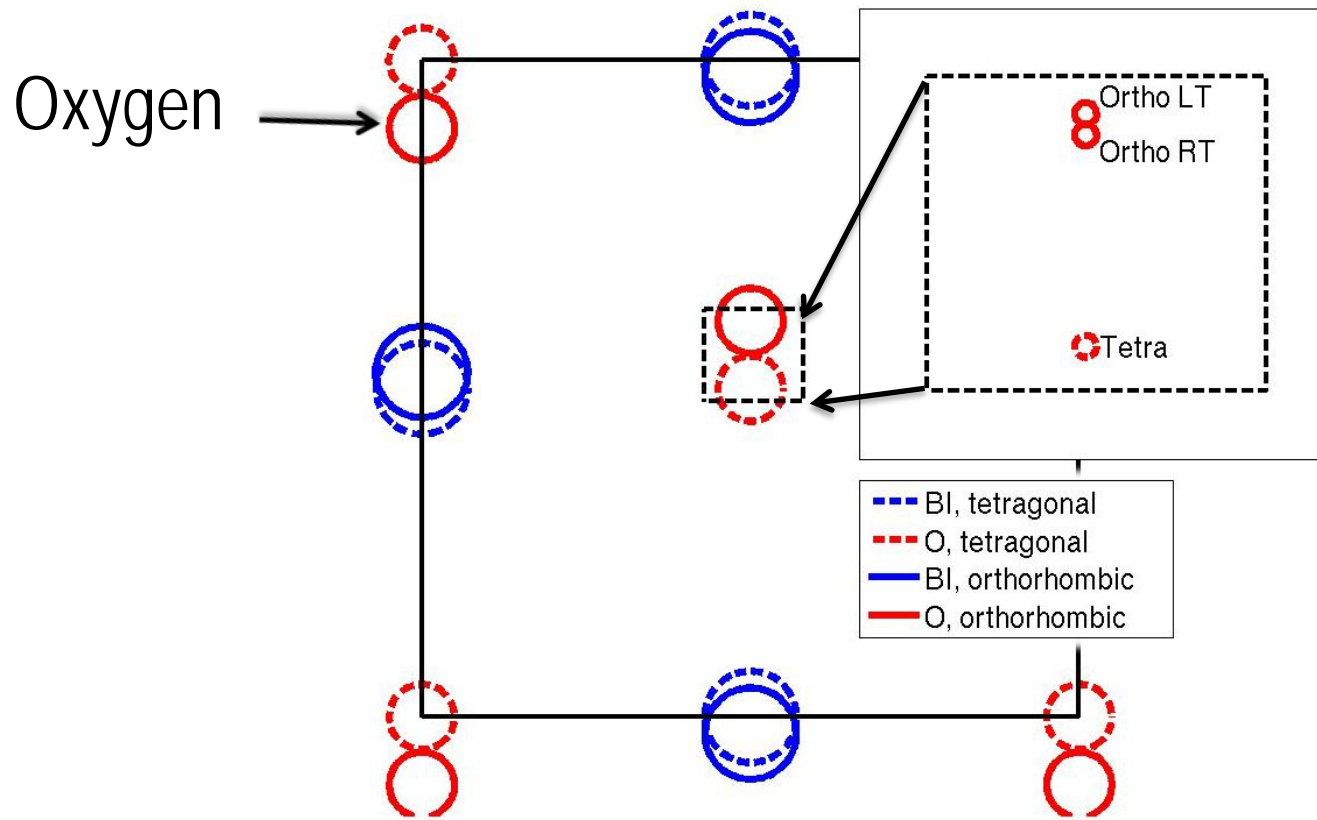
We report first-principles computations of the angle-resolved photoemission response with circularly polarized light in  $\text{Bi}_2\text{Sr}_2\text{CaCu}_2\text{O}_{8+\delta}$  for the purpose of delineating contributions to the circular dichroism resulting from distortions and modulations of the crystal lattice. Comparison with available experimental results shows that the measured circular dichroism from antinodal mirror planes is reproduced in quantitative detail in calculations employing the average orthorhombic crystal structure. We thus conclude that the existing angle-resolved photoemission measurements can be understood essentially within the framework of the conventional picture, without the need to invoke unconventional mechanisms.

# Possible origins of the symmetry breaking in mirror plane

- Geometry i.e. there is no mirror plane due to e.g. orthorhombic crystal structure.
- Time reversal symmetry breaking due to :
  - Orbital currents and related dynamic effects.
  - Spin related effects.

Next we will explore how sensitive  $D_S$  is to geometrical symmetry breaking.

# Shifts in atomic position due to temperature in BiO -layer



# Orthorhombic

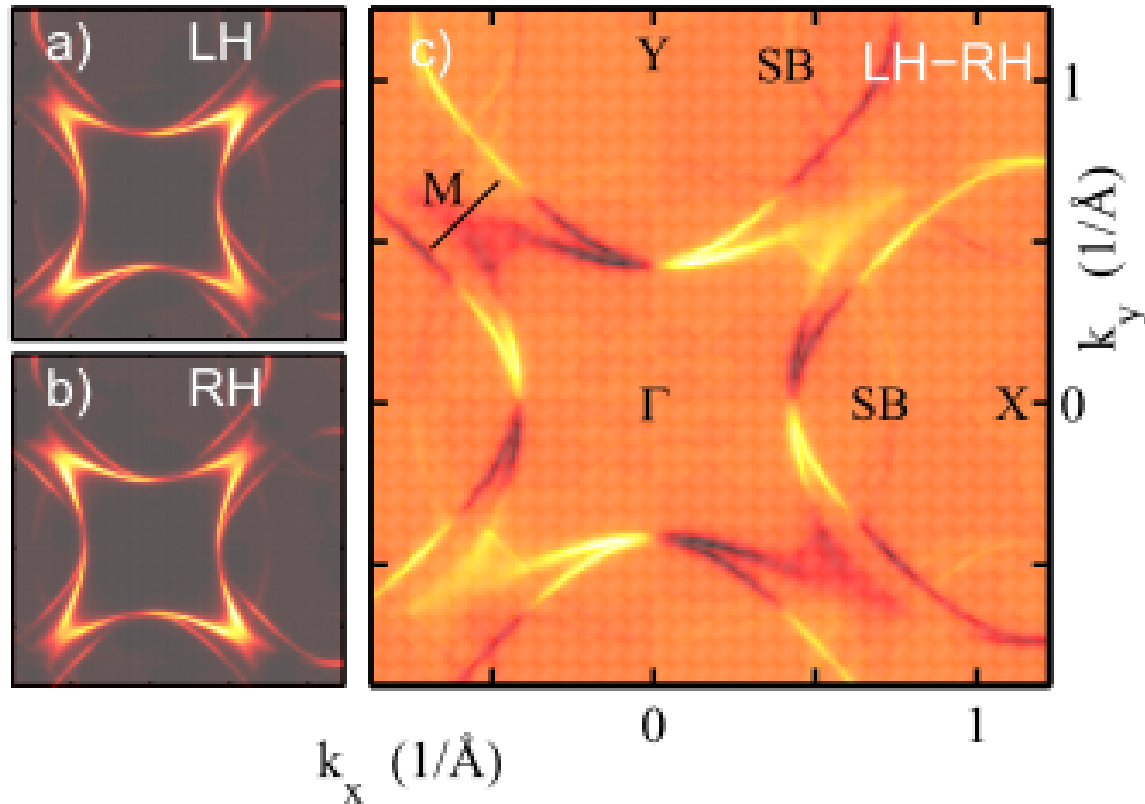
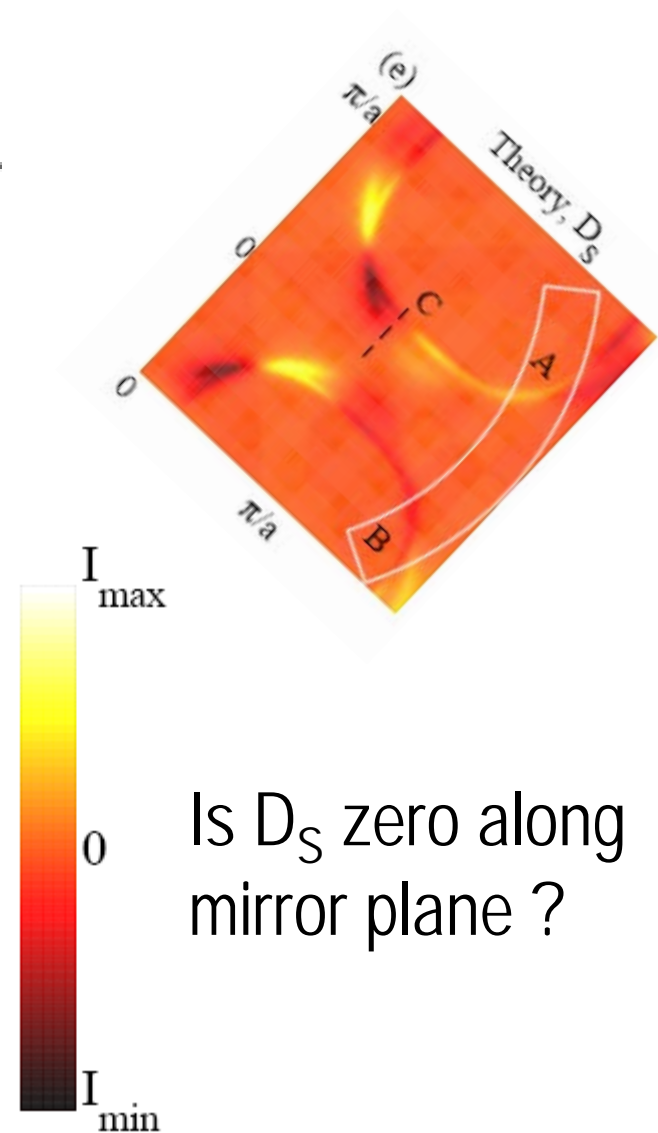
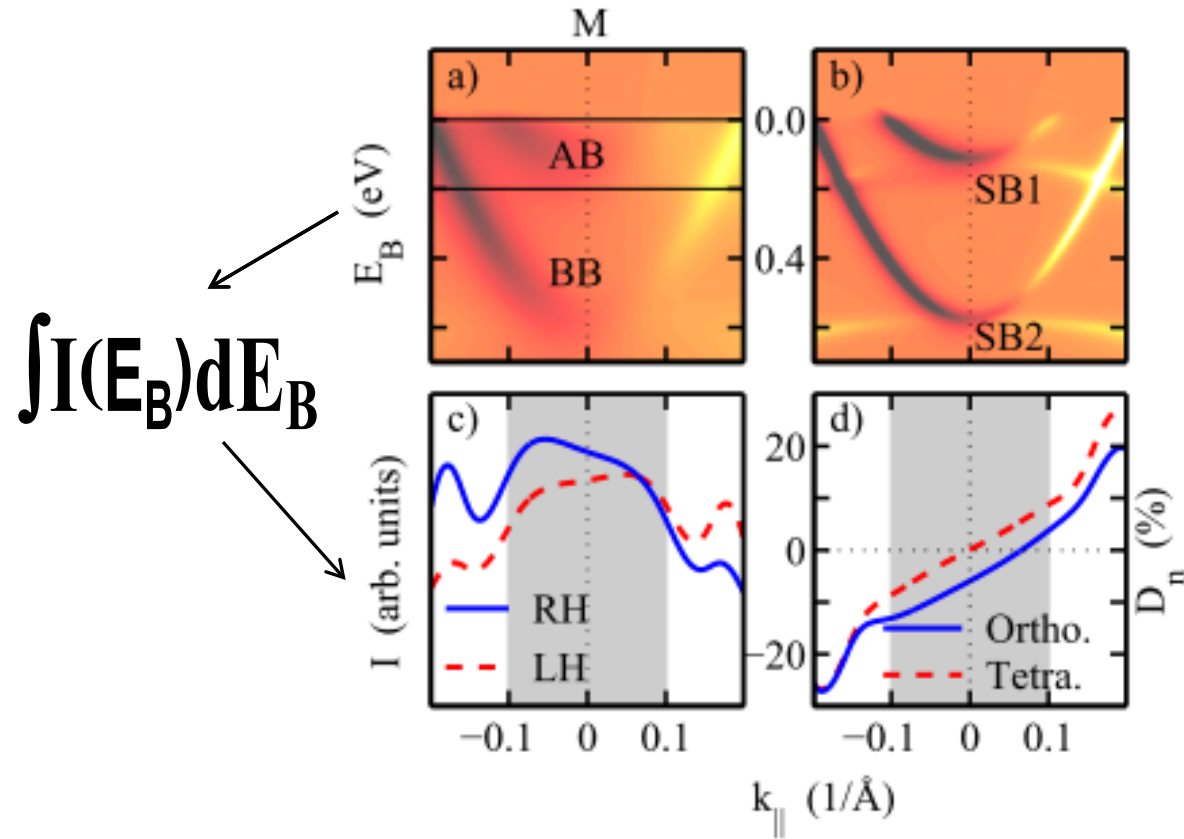


FIG. 1: (Color online) Theoretically obtained photo-intensity in orthorhombic Bi2212 for emission from the Fermi energy using 21 eV light incident normally to the surface. (a) Left-handed (LH) polarized light; (b) Right-handed (RH) polarized light; and, (c) Dichroic intensity obtained by taking the difference (LH-RH) of the maps in (a) and (b). Black denotes low and white denotes high intensity.

# Tetragonal



Is  $D_s$  zero along mirror plane ?



Effect of the  
shadow bands

FIG. 2: (Color online) Computed dichroic intensity at and near the  $M(\pi,0)$  symmetry point. (a) Dichroic intensity as a function of binding energy for momenta along the black line in Fig. 1(c). Horizontal axis denotes  $k_{\parallel}$  distance from the M-point, where  $k_{\parallel} = 0$  is the M-point. (b) Same as (a), except this panel corresponds to a very small initial state width to highlight various spectral features (AB, BB, SB) discussed in the text. (c) Spectral weight integrated over the binding energy range of 0-0.2 eV (pair of black horizontal lines in (a)) for RH and LH polarized light. (d) Normalized dichroic signal  $D_n$ , energy-integrated over the 0-0.2 eV binding energy range, for the orthorhombic and tetragonal structures.

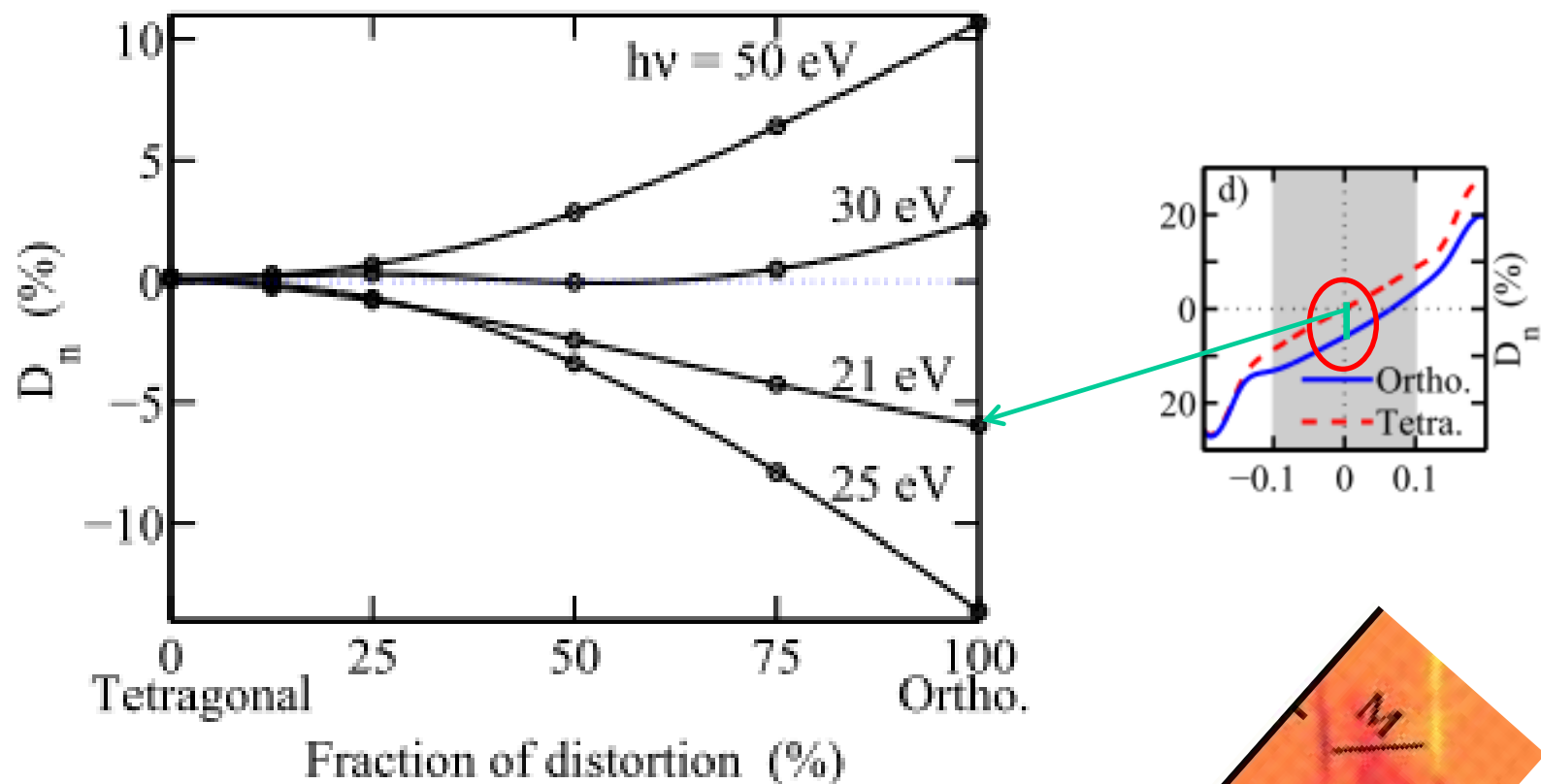


FIG. 3: Energy-integrated dichroic weight  $D_n$  at the M-point as a function of geometric distortion. Horizontal axis gives the fractional (in percent) movement of the atoms in going from the tetragonal to the experimental orthorhombic structure at 12K. Smooth lines have been drawn through the computed points.



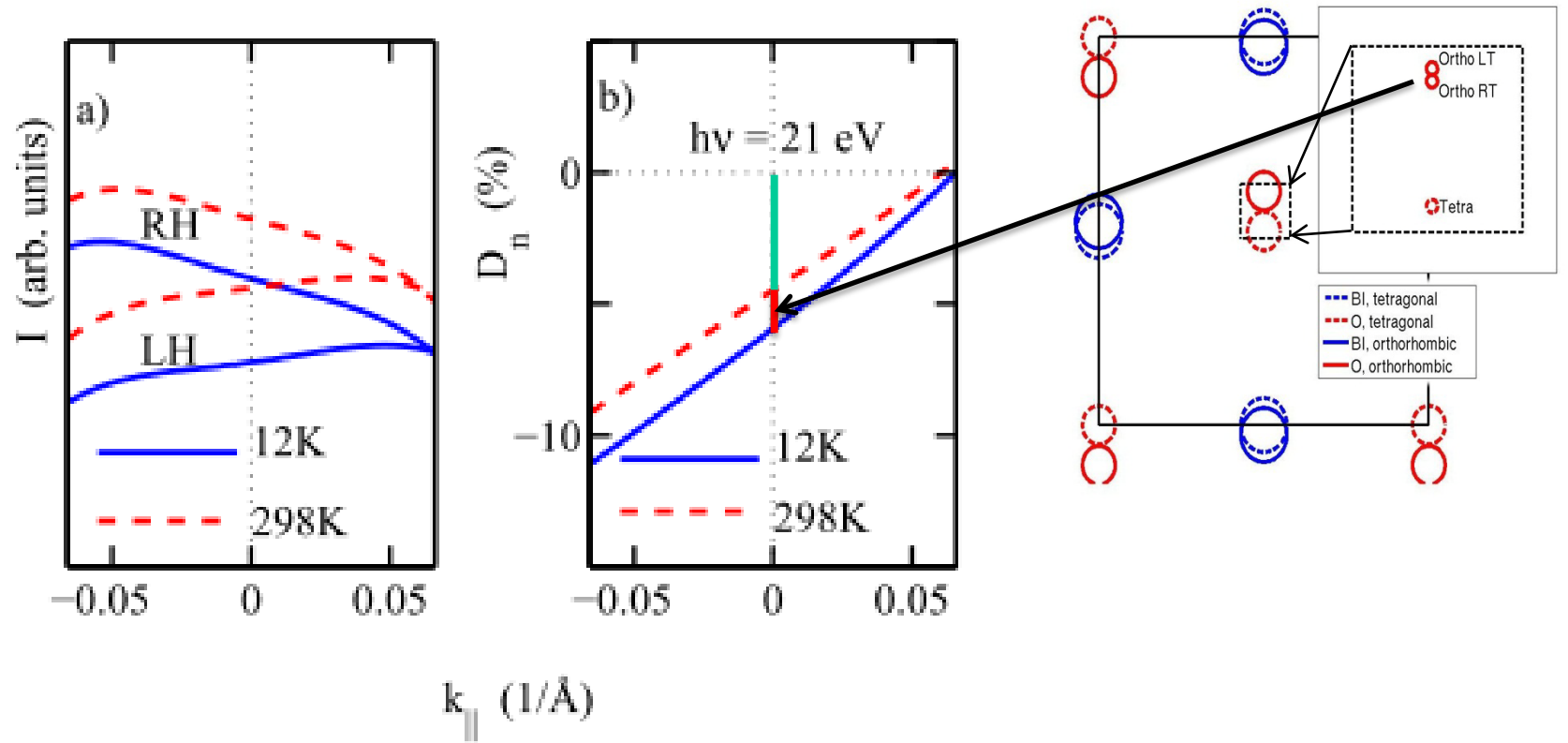


FIG. 4: (Color online) (a) Computed energy-integrated intensity in Bi2212 near the M-point for the experimentally refined orthorhombic structures at 12K (solid red and blue lines) and 298K (dashed blue and red lines) of Ref. 13. Horizontal axis is the same as in Fig. 2 except for a narrower momentum range with  $k_{\parallel} = 0$  corresponding to the M-point. Results are for LH and RH polarized light at 21 eV. (b) Dichroic signal obtained by taking the difference LH-RH from the results in (a).

TABLE I: Computed values of the energy-integrated dichroic intensity  $D_n$  (in percent) at the M-point for low- and room-temperature orthorhombic structure of Bi2212 at three different photon energies  $\hbar\nu$  are compared with the available measurements. Experimental results are from Ref. 7 for a thin film sample, and from Ref. 9 for samples with O- and Pb-doping.

	Theory			Experiment		
				Single crystal <sup>9</sup>	Thin film <sup>7</sup>	Lead- doped <sup>9</sup>
$\hbar\nu$ (eV)	21	30	49.7	49.7	21	49.7
$D_n$ (%) at 298K	4.5	1	6	5	0	0
$D_n$ (%) at 12K	6	2.5	9.5		3	0

<sup>7</sup> A. Kaminski et al., Nature **416**, 610 (2002).

<sup>9</sup> S. V. Borisenko et al., Nature **431**,  
doi:10.1038/nature02931 (2004).

# Conclusions

We can compute ARPES intensity excited by circularly polarized light with reasonable results

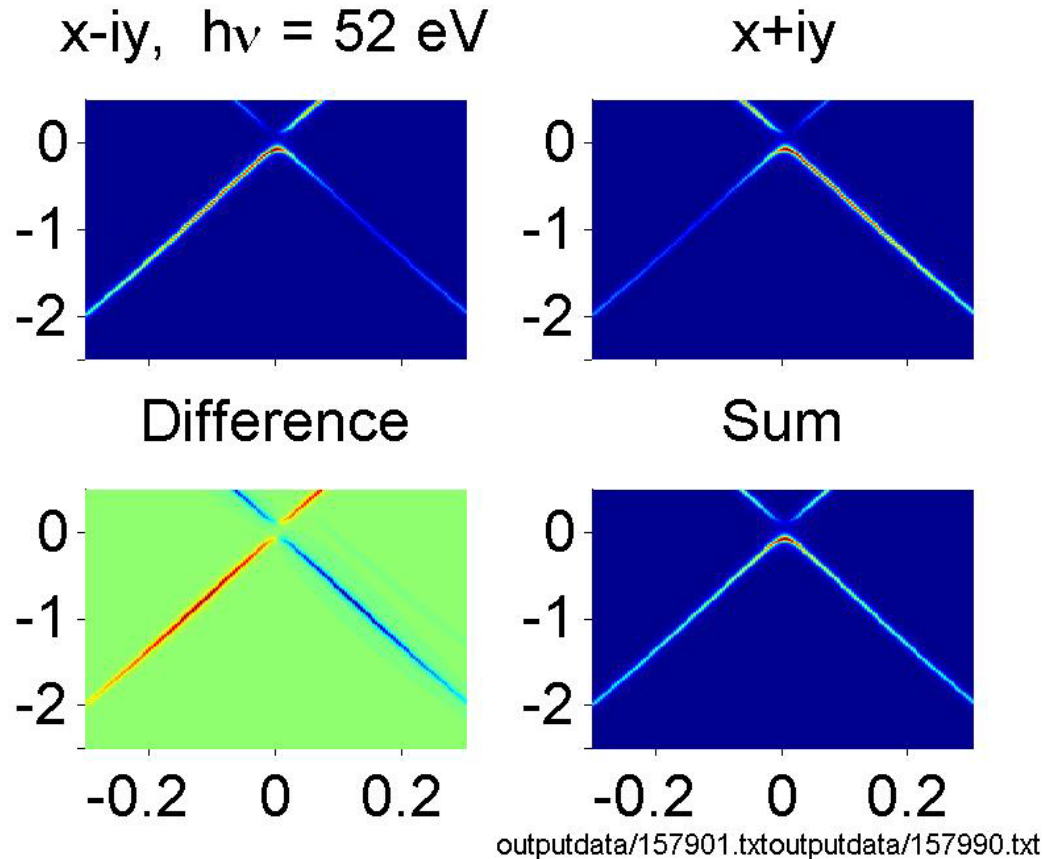
Comparison with available experimental results shows that the measured dichroism from antinodal mirror planes is reproduced in quantitative detail in computations employing the average orthorhombic crystal structure.

# Graphene

# What can be computed?

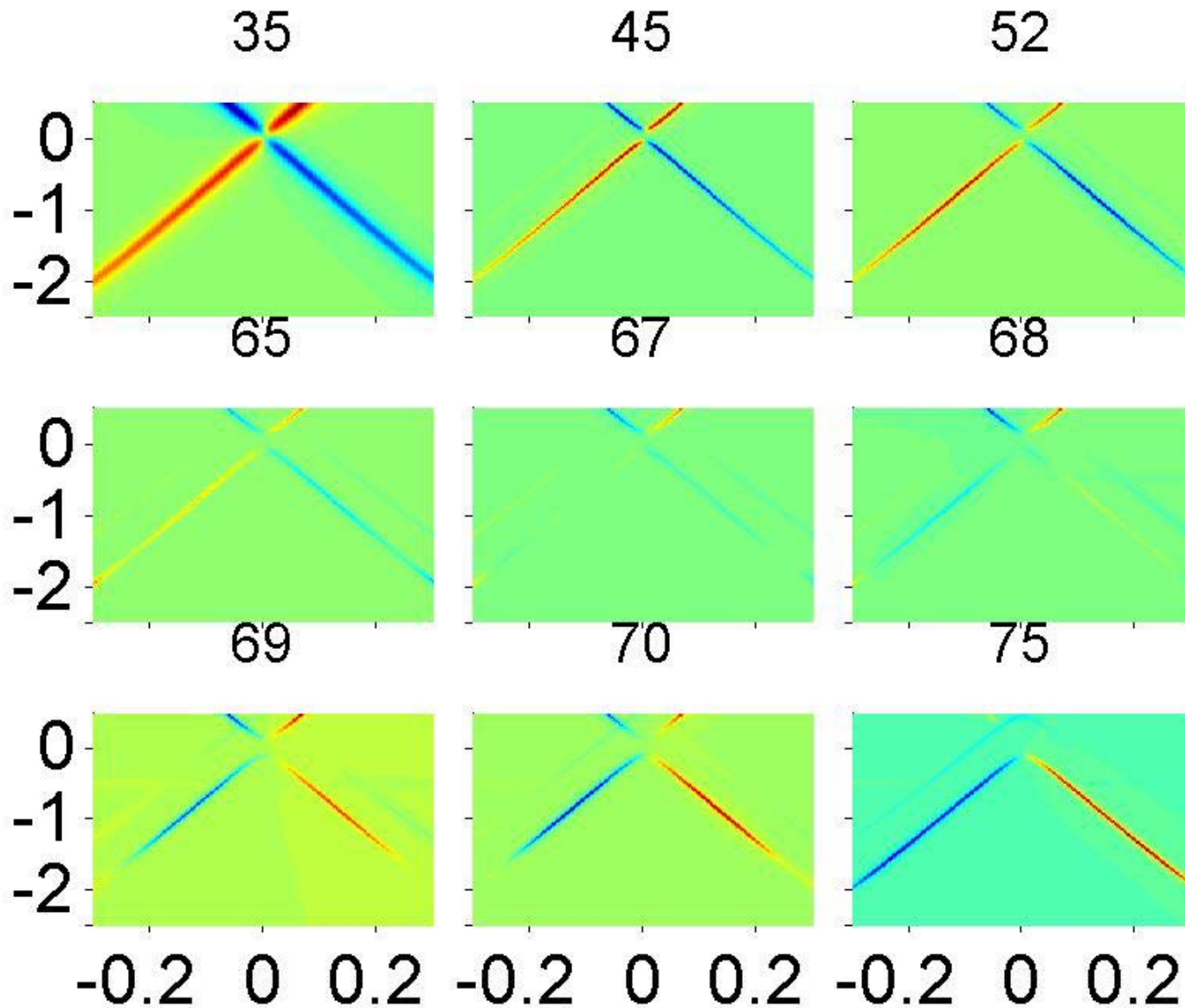
- Momentum Distribution Curves.
- Constant Initial State Maps

# Momentum Distribution Curves

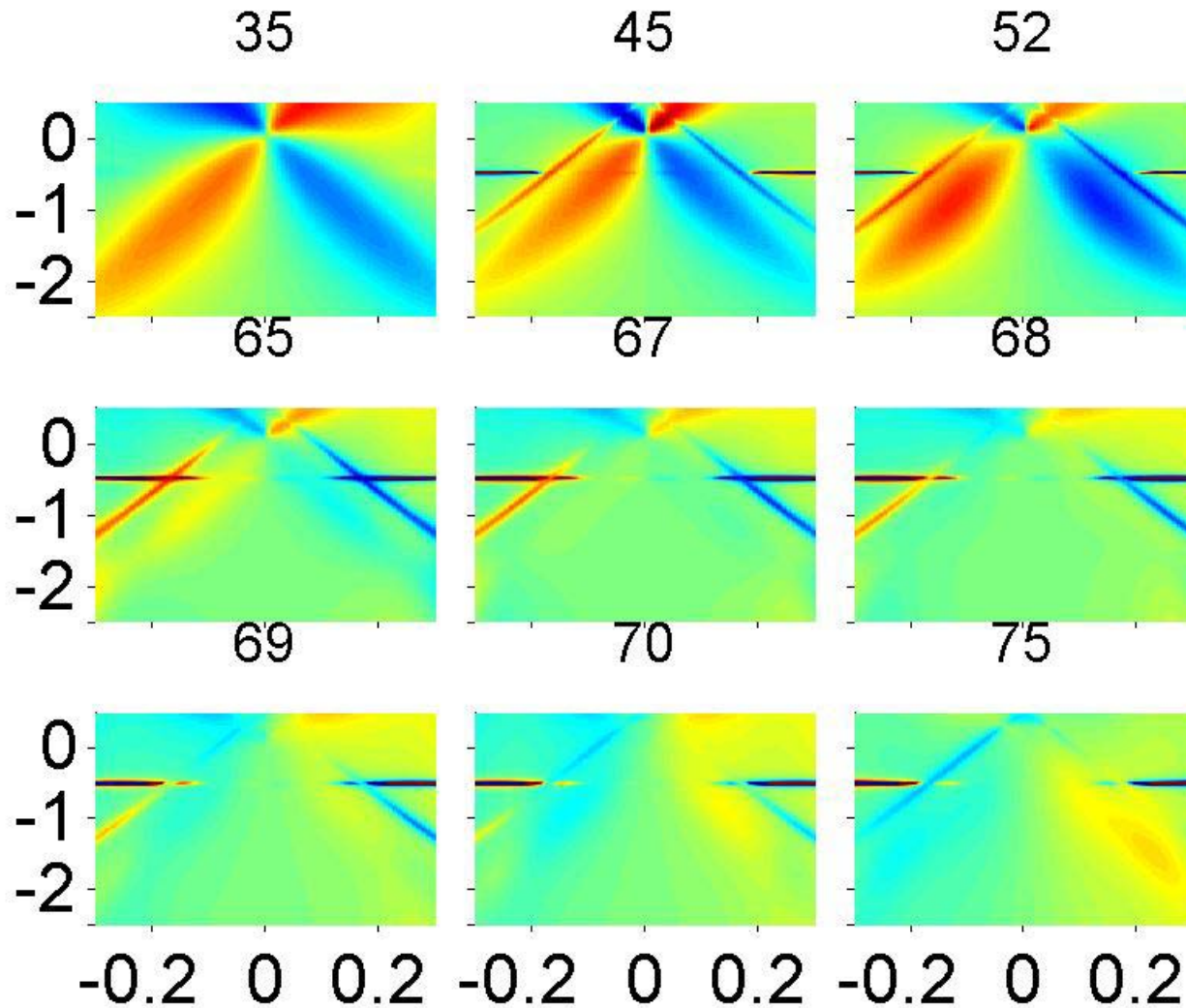


Note momentum of the incoming light (no gap at K).

# Difference set as a function of Photon energy



# Normalized dichromatic signal

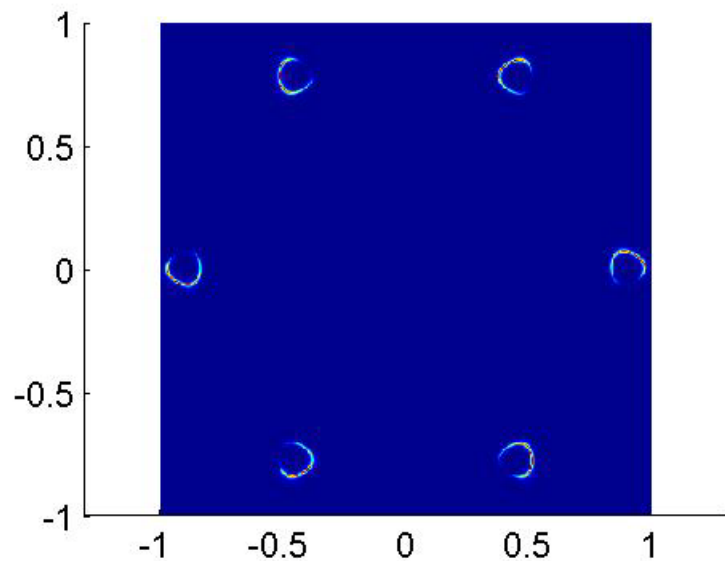


Normalization is tricky...

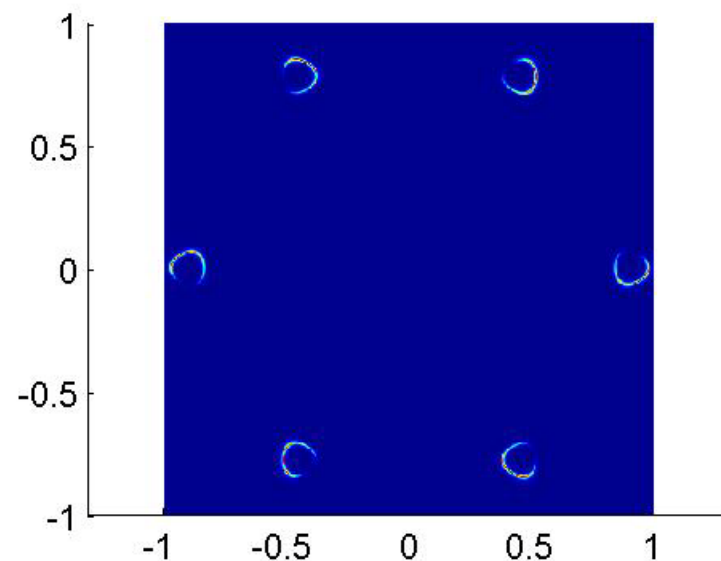


We can compute constant initial  
state maps (Fermi surface maps)

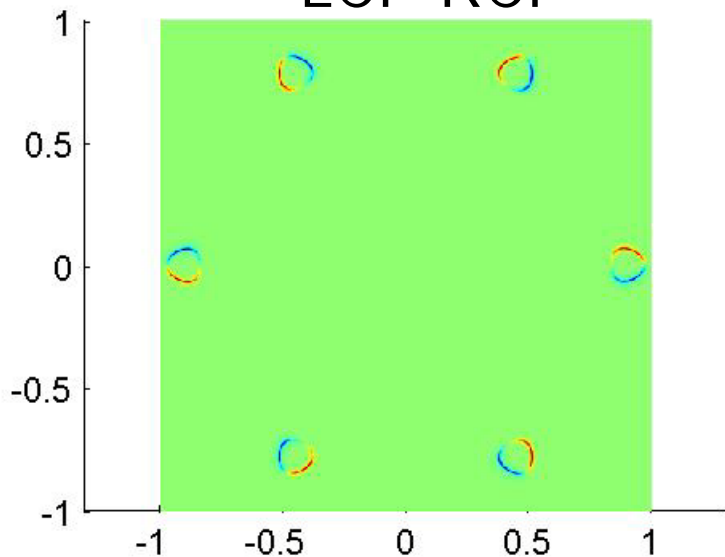
LCP



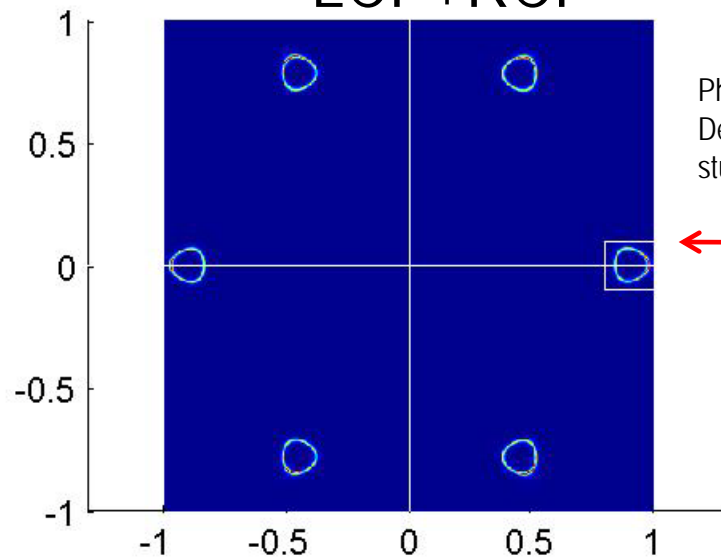
RCL



LCP-RCP



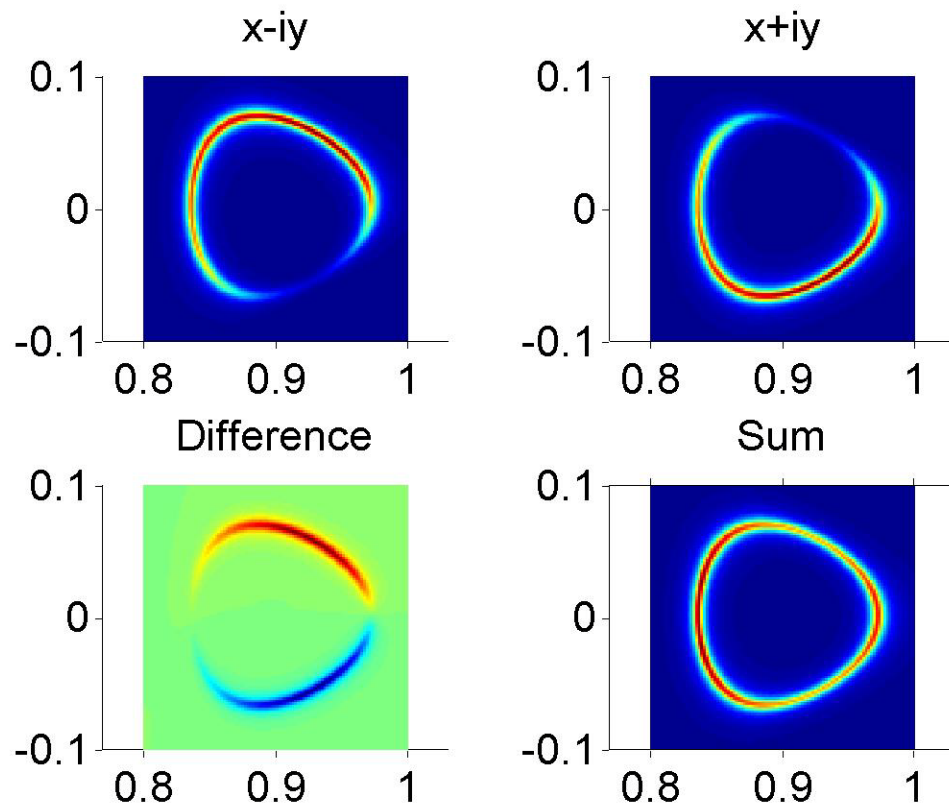
LCP+RCP



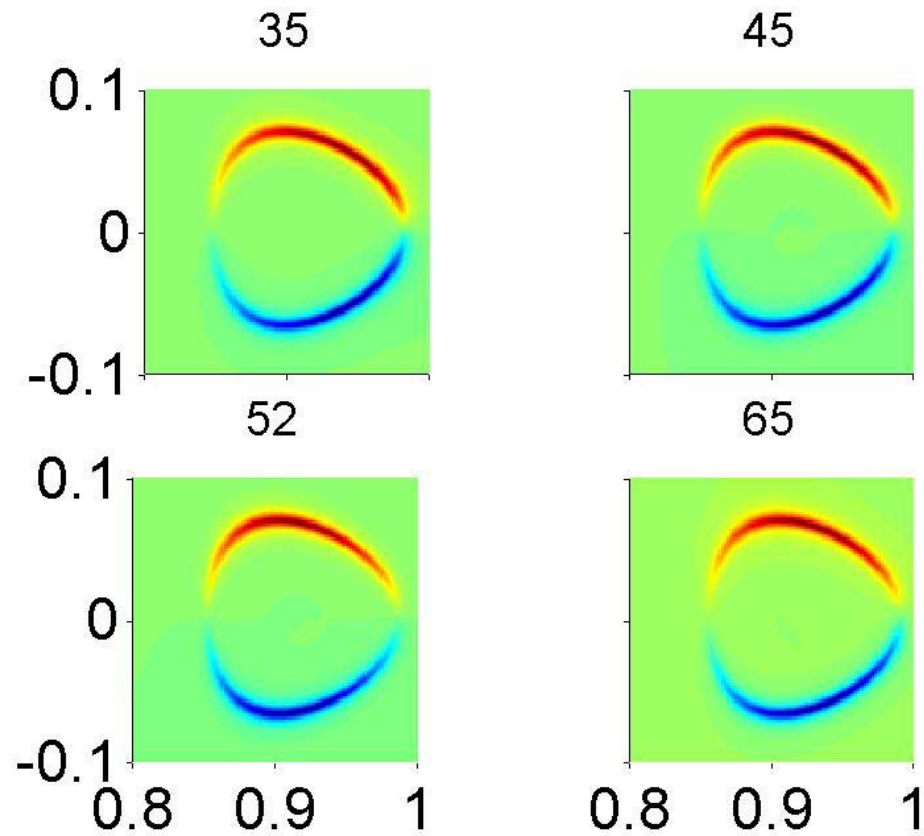
Photon energy  
Dependence  
studied

150787.txt 1\*\*\* 34kkgraphene4.pot fermi35p.dat empty.sati Sun Feb 6 13:31:16 2011  
4.6487-0.2144-0.2078-0.0010-0.1470 0.0000 0.0000 0.5000 0.0000 1.0000 1.0000 0.0000 0 80 2  
-0.19 -1 -1 1.2863 0 0 0 0.00025749

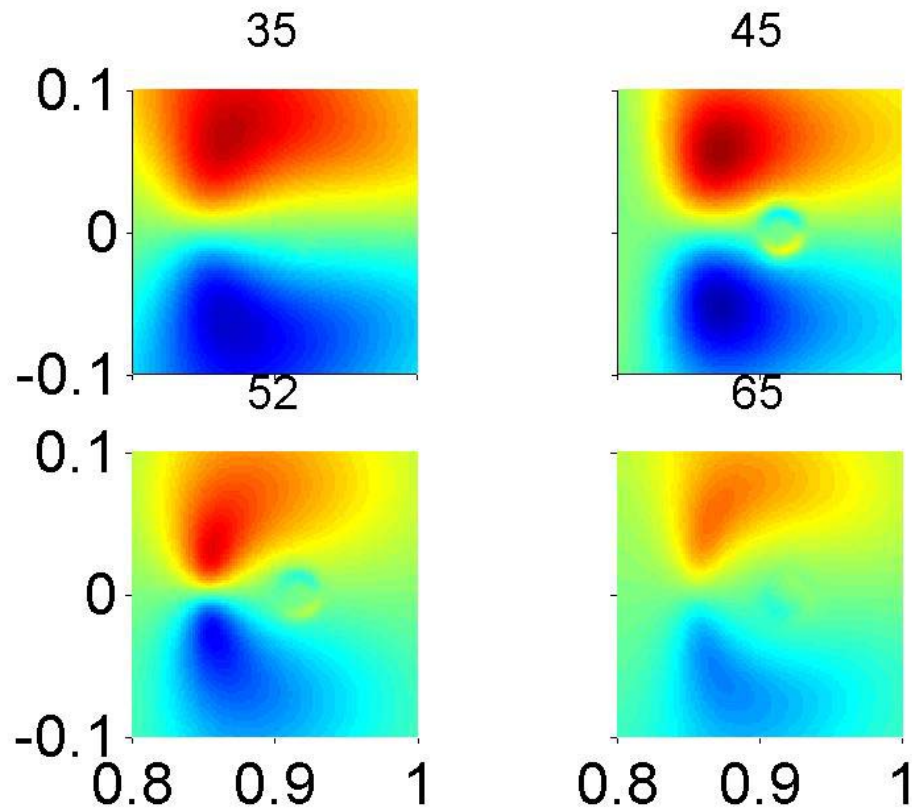
# Computed dicromatic signals



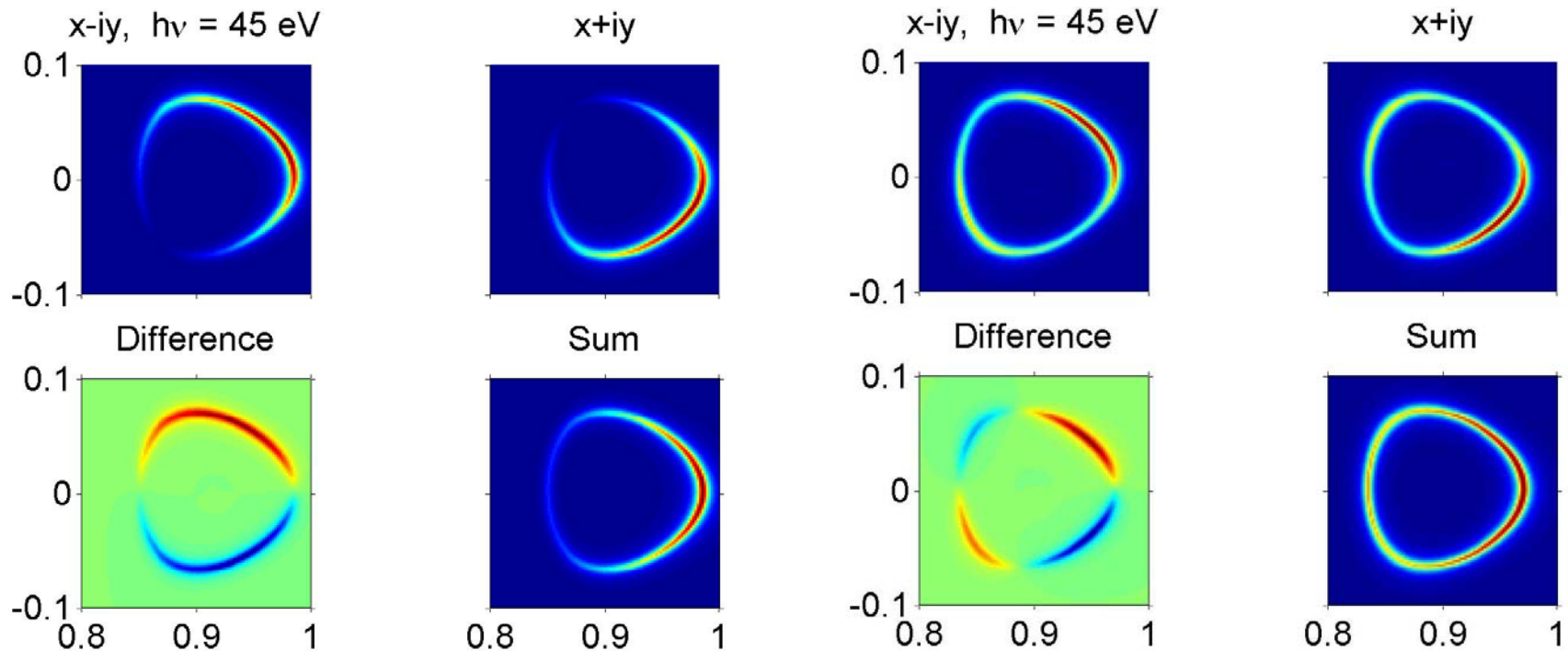
# Differences



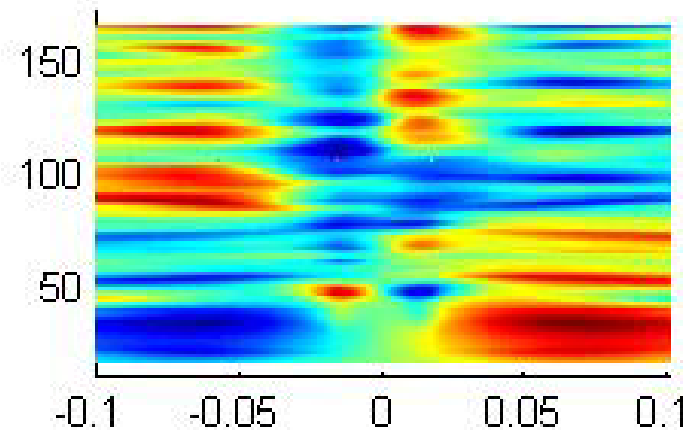
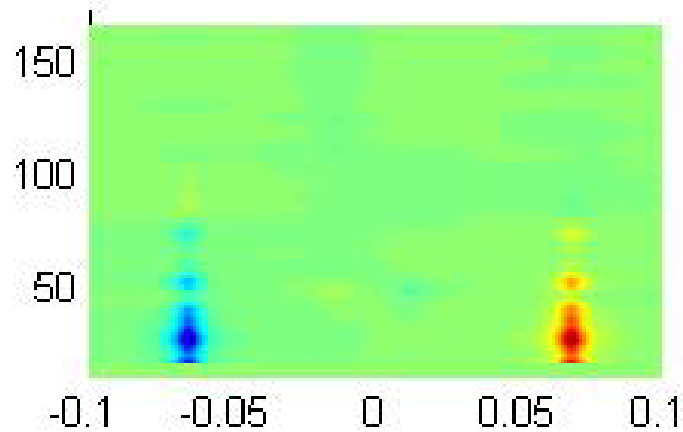
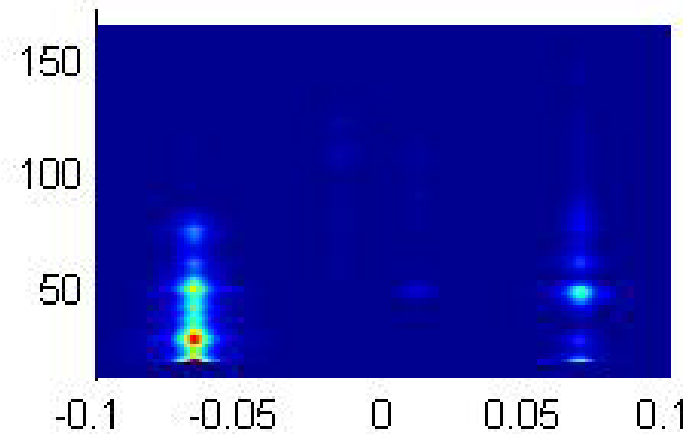
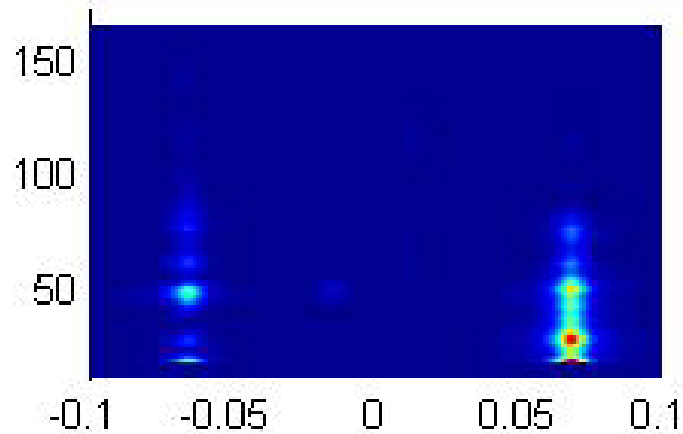
# Normalized dichromatic signal...



# Different polar angle for light...



# Photon energy dependence



# Graphene Sublattice Symmetry and Isospin Determined by Circular Dichroism in Angle-Resolved Photoemission Spectroscopy

Isabella Gierz,<sup>\*,†,⊥</sup> Matti Lindroos,<sup>‡</sup> Hartmut Höchst,<sup>§</sup> Christian R. Ast,<sup>†</sup> and Klaus Kern<sup>†,||</sup>

<sup>†</sup>Max-Planck-Institut für Festkörperforschung, D-70569 Stuttgart, Germany

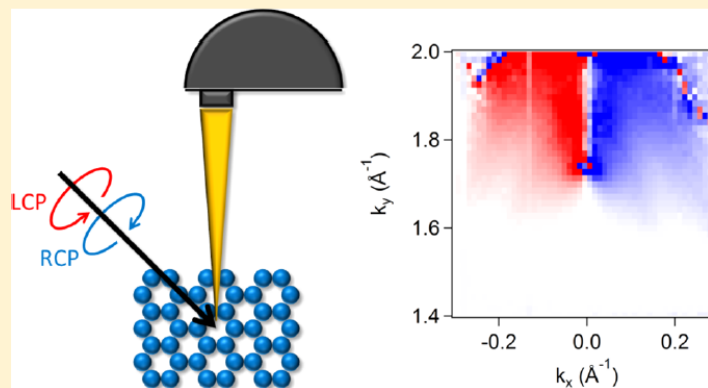
<sup>‡</sup>Department of Physics, Tampere University of Technology, 33101 Tampere, Finland

<sup>§</sup>Synchrotron Radiation Center, University of Wisconsin-Madison, Stoughton, Wisconsin 53589, United States

<sup>||</sup>Institut de Physique de la Matière Condensée, Ecole Polytechnique Fédérale de Lausanne, CH-1015 Lausanne, Switzerland

**ABSTRACT:** The Dirac-like electronic structure of graphene originates from the equivalence of the two basis atoms in the honeycomb lattice. We show that the characteristic parameters of the initial state wave function (sublattice symmetry and isospin) can be determined using angle-resolved photoemission spectroscopy (ARPES) with circularly polarized synchrotron radiation. At a photon energy of  $h\nu = 52$  eV, transition matrix element effects can be neglected allowing us to determine sublattice symmetry and isospin with high accuracy using a simple theoretical model.

**KEYWORDS:** Graphene, sublattice symmetry, isospin, circular dichroism, ARPES





graphene lattice has two carbon atoms per unit cell, the  $\pi$ -bands consist of two  $p_z$ -orbitals that are either centered on atom A or on atom B. Therefore, we write the initial state wave function as  $|\Psi_i\rangle = c_A|p_z, A\rangle \pm c_B|p_z, B\rangle$ , where the coefficients  $c_A$  and  $c_B$  fulfill  $|c_A|^2 + |c_B|^2 = 1$  and  $c_B/c_A = Ae^{i\theta_k}$ <sup>10</sup> with  $A = 1$  ( $A \neq 1$ ) for equivalent (inequivalent) sublattices. The  $+$  ( $-$ ) sign corresponds to the conduction (valence) band. Further, we assume that  $\langle\Psi_f|H|p_z, B\rangle = e^{-i\phi_0} \langle\Psi_f|H|p_z, A\rangle$ . The phase factor  $e^{-i\phi_0}$  describes the phase difference between electrons emitted from sublattice A and B, respectively, and has been inserted to account for the experimentally observed rotation of the dark corridor with photon energy. In the following, we will skip the subscript A in  $|p_z, A\rangle$  and write  $|p_z\rangle$  instead. For our present purpose we do not need to make any assumption about the final state wave function  $\Psi_f$ . In this case the photocurrent is given by

$$I \propto |\langle\psi_f|H|\psi_i\rangle|^2 = \left(1 \pm \frac{2A}{1 + A^2} \cos(\theta_k - \phi_0)\right) |\langle\psi_f|H|p_z\rangle|^2$$

the normalized CDAD signal,  $I_{\text{nCDAD}} =$

$$\frac{\pm A(\cos(\phi - \phi_{\text{RCP}}) - \cos(\phi - \phi_{\text{LCP}}))}{1 + A^2 \pm A(\cos(\phi - \phi_{\text{RCP}}) + \cos(\phi - \phi_{\text{LCP}}))} \quad (2)$$

where  $\phi_{\text{RCP,LCP}}$  is the position of the dark corridor for RCP and LCP light, respectively.

the context of Figure 4c. Thus we conclude that for  $h\nu = 52$  eV the assumption that  $|\langle \Psi_f | H | p_z \rangle|^2 \approx \text{constant}$  within the region of interest around the  $\bar{\text{K}}$ -point holds, which means that the experimental data is mainly determined by the initial state (blue). By fitting this data to the model in eq 1 we can determine the position of the dark corridor for RCP and LCP light,  $\phi_{\text{RCP}} = (6 \pm 1^\circ)$  and  $\phi_{\text{LCP}} = (-17 \pm 1^\circ)$ . The fits are different radial distances from the  $\bar{\text{K}}$ -point. The resulting data points (open black spheres) can be nicely fitted to the model in eq 2 with  $A = 1.0 \pm 0.1$  (see continuous line in Figure 4c). In choice of the photon energy). Thus, we are able to determine the parameters  $c_A$  and  $c_B$  in the initial state wave function of graphene as  $|c_{A,B}|^2 = (0.50 \pm 0.05)$  and  $c_B = (1.0 \pm 0.1)c_A e^{i\phi}$ .

## Reversal of the Circular Dichroism in Angle-Resolved Photoemission from $\text{Bi}_2\text{Te}_3$

M. R. Scholz,<sup>1,\*</sup> J. Sánchez-Barriga,<sup>1</sup> J. Braun,<sup>2</sup> D. Marchenko,<sup>1</sup> A. Varykhalov,<sup>1</sup> M. Lindroos,<sup>3</sup> Yung Jui Wang,<sup>4</sup>  
Hsin Lin,<sup>4</sup> A. Bansil,<sup>4</sup> J. Minár,<sup>2</sup> H. Ebert,<sup>2</sup> A. Volykhov,<sup>5</sup> L. V. Yashina,<sup>5</sup> and O. Rader<sup>1</sup>

<sup>1</sup>*Helmholtz-Zentrum Berlin für Materialien und Energie, Elektronenspeicherring BESSY II, Albert-Einstein-Strasse 15,  
12489 Berlin, Germany*

<sup>2</sup>*Department Chemie, Ludwig-Maximilians-Universität München, Butenandtstrasse 5-13, 81377 München, Germany*

<sup>3</sup>*Institute of Physics, Tampere University of Technology, P.O. Box 692, 33101 Tampere, Finland*

<sup>4</sup>*Physics Department, Northeastern University, Boston, Massachusetts 02115, USA*

<sup>5</sup>*Department of Chemistry, Moscow State University, Leninskie Gory 1/3, 119992 Moscow, Russia*  
(Received 4 July 2012; revised manuscript received 9 March 2013)

The helical Dirac fermions at the surface of topological insulators show a strong circular dichroism which has been explained as being due to either the initial-state spin angular momentum, the initial-state orbital angular momentum, or the handedness of the experimental setup. All of these interpretations conflict with our data from  $\text{Bi}_2\text{Te}_3$  which depend on the photon energy and show several sign changes. Our one-step photoemission calculations coupled to *ab initio* theory confirm the sign change and assign the dichroism to a final-state effect. Instead, the spin polarization of the photoelectrons excited with linearly polarized light remains a reliable probe for the spin in the initial state.

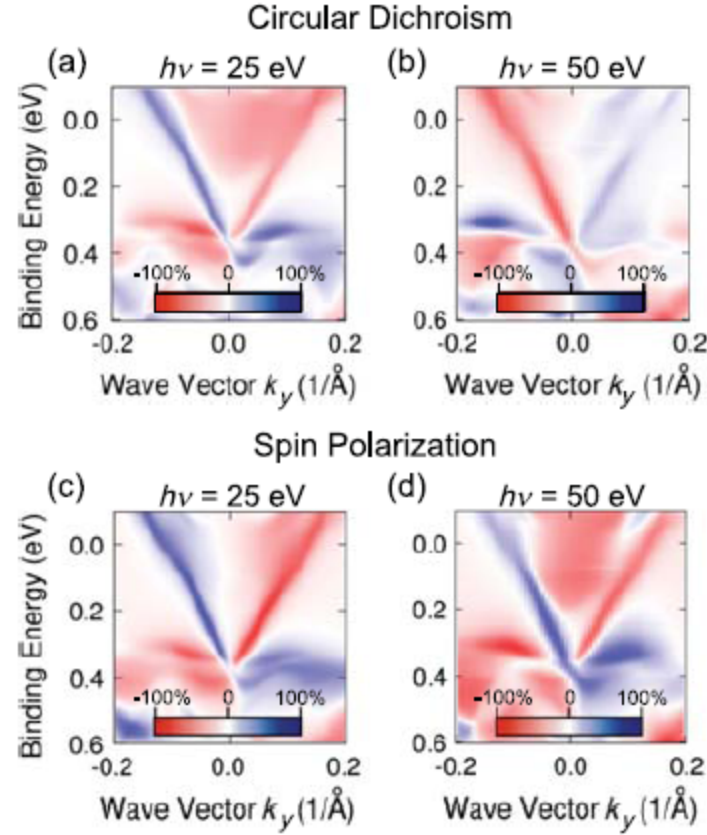


FIG. 4 (color online). Results from the one-step photoemission calculation. Top: Calculated circular dichroism changes sign between photon energies of (a) 25 eV and (b) 50 eV. Bottom: For the same system but linearly polarized light. The calculated spin polarization  $P$  of the photoemission from the topological surface state is unaffected by the photon energy. It reaches  $P \sim 80\%$  at 25 eV in (c) and  $75\%$  at 50 eV in (d).

# Conclusions

- Computations of circular dichromatic signal is as possible as computations of ARPES excited by linearly polarized light. It only take twice amount of time.
- Studies of circular dichromatic signals are relative uncharted territory and many interesting new things could be found there.

Thank you

Questions ?